Jurnal Teknologi

Full paper

Effects of Aluminosilicate Mineral Nano-Clay Fillers on Polysulfone Mixed Matrix Membrane for Carbon Dioxide Removal

Oh P.C.*, Mansur N. A.

Department of Chemical Engineering, Universiti Teknologi PETRONAS, Bandar Seri Iskandar, 31750 Perak, Malaysia

*Corresponding author: peiching.oh@petronas.com.my

Article history

Received :15 September 2013
Received in revised form :
17 November 2013
Accepted :15 January 2014

Graphical abstract

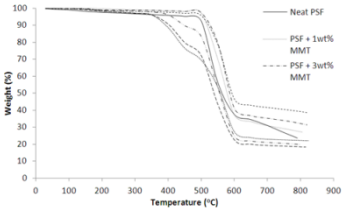

Abstract

Over the last few decades, significant improvements in the performance of polymeric membranes for gas separation have been made. Nevertheless, the existing membrane materials need to be enhanced in order to fully exploit their gas separation application opportunities on industrial scale. Mixed matrix membrane which combines the advantages of the highly selective fillers and desirable properties of the polymer matrix is explored to overcome the trade-off trend between gas permeability and selectivity. This paper describes the effect of aluminosilicate mineral nano-clay fillers on polysulfone (PSF) mixed matrix membrane. In this study, different types of montmorillonite (MMT) nano-clays were used as fillers to fabricate asymmetric flat sheet mixed matrix membrane (MMM) via dry-wet phase inversion method. The interaction between the type of organoclay and its loading is also studied. The synthesis of MMM required *N*-methyl-2-pyrrolidone (NMP) as solvent and deionized water as coagulant. The fabricated MMMs were characterized by thermal gravimetric analysis (TGA), differential scanning calorimetry (DSC) and field emission scanning electron microsropy (FESEM). Thin asymmetric membrane with dense skin layer and porous sub-structure was successfully fabricated. Results showed enhancement in MMM stability relative to neat PSF membrane. It is also found that higher nano-clay loading resulted in significant agglomeration, nevertheless, there appears to be improved adhesion between the polymer and nano-clay.

Keywords: Polysulfone; aluminosilicate; montmorillonite; mixed matrix membrane

1.0 INTRODUCTION

Membrane technology for separation of CO_2 from natural gas is an important industry worth millions of dollars [1]. To date, researchers strive to develop membrane materials that could produce high fluxes, great selectivity and permeability [2,3]. According to Susanto and Unbricht (2009), polymeric membranes are still dominantly used in many industrial applications due to availability of materials for commercial use, extensive polymer properties and cost effectiveness [4].

Despite these advantages, polymeric membranes are still restricted by the trade-off trend between gas permeability and selectivity, as suggested by Robeson [5]. Therefore, alternate approaches that can enhance their gas separation properties well above the Robeson line are needed [6].

Mixed matrix membranes (MMMs), herein defined as inorganic nanofillers dispersed in a polymer matrix, possess the potential to solve the trade-off problem of polymeric membranes. This is due to the fact that MMMs may combine the advantages of the polymeric material and inorganic fillers, thus, incorporating the flexibility and processability of the polymers together with the selectivity and thermal stability of the inorganic fillers. A wide range of nanofillers such as layered silicates (clays), zeolites and carbon molecular sieves have been utilized for a variety of applications. Nevertheless, the main concern for fabrication of MMMs remains: the selection of suitable polymer-inorganic components and elimination of interfacial defects between the two phases for attaining homogeneity so that phase separation can be avoided [7].

Polysulfone (PSF) is a well-known membrane material for gas separation due to its excellent film forming capability as well as mechanical restraint and thermal stability [8]. This glassy polymer has demonstrated great diffusion selectivity for CO_2/CH_4. Montmorillonite (MMT), a type of swelling clay, has been employed predominantly in the synthesis of polymer-clay nanocomposite since it is a natural occurring mineral that is commercially available, inexpensive, and demonstrates platy morphology. The platelet structure of this aluminosilicate material has proven to enhance barrier properties of polymeric material [9].

Hence, this research aimed to prepare PSF/MMT mixed matrix membranes by phase inversion method using different types of aluminosilicate mineral nano-clay fillers (raw MMT and surface modified MMT). Effects of nano-clay chemical composition and nano-clay content on the morphology and thermal properties of the MMMs were investigated. By

understanding the morphology and physical features, the performance of the membrane can be predicted. The synthesized PSF/MMT membranes were subsequently characterized by using various analytical tools. To the best of our knowledge, there is no documentation on the use of these two types of MMT with polysulfone in MMM for gas separation application.

2.0 EXPERIMENTAL

2.1 Raw materials

A commercial Udel® Polysulfone, purchased from Solvay Advanced Polymers was used as the polymer matrix. *N*-methyl-2-pyrrolidone (NMP) supplied by Merck was used as the solvent, while deionized water was used as the non-solvent. The raw MMT and Nanomer 1.34TCN (surface modified MMT with 25%–30% of methyl dihydroxyethyl hyrogenated tallow-ammonium) were purchased from Sigma Aldrich. All materials were used without further purification. Henceforth, raw MMT and organomodified MMT are denoted as MMT and O.MMT respectively.

2.2 Fabrication of Asymmetric Flat Sheet Mixed Matrix Membrane

In this paper, three types of membranes were prepared; neat PSf membrane, PSF/MMT MMM, and PSF/O.MMT MMM. The casting dope was prepared by mixing 25wt% of PSF polymer with 75wt% NMP. Then, different MMT concentration (0wt%, 1wt%, 3wt%, and 5wt%) was added to the casting solution and stirred at 50°C until the polymer and clay dissolved completely in the solution. The solution was further stirred for 24 hours at room temperature to ensure complete dissolution of polymer and clay. The mixed solution was degassed by using ultrasonic degasser for at least 4 hours to remove trapped air bubbles, and then left standing for 1 day. Longer degassing duration might be necessary for casting dope with higher clay loading.

Flat sheet asymmetric membrane was prepared through dry-wet phase inversion method. Before casting, the mixture was further sonicated for 30 minutes and left standing for another 30 minutes to ensure homogenous dispersion of clay. The degassed solution was then poured onto a flat, leveled glass plate, cast into a thin film with a casting knife at a gap setting of 225µm at an appropriate casting shear. The cast solution is slowly evaporated at ambient condition for 15 minutes. Then, the film is immersed in an aqueous bath at 25°C. During this process, solvent exchange occurred, followed by solidification of the membrane film. To ensure that the solvent was fully removed, the membrane was left in the bath for 1 day. Finally, the membrane was washed with distilled water and dried for 24 hours at 60°C. The procedure is repeated for preparing MMMs with organically surface modified MMT (O.MMT) at 1wt%, 3wt% and 5wt% clay concentration.

2.3 Mixed Matrix Membrane Characterization

Thermal gravimetric analysis (TGA) was performed on the pristine PSF membrane and MMMs using a thermogravimetric analyzer (Model: Perkin Elmer TGA-7). The samples were heated from 30 to 800°C at a heating rate of 10°C min^{-1}, under nitrogen atmosphere, with a nitrogen flow rate of 50 mL min^{-1}.

The glass transition temperature (T_g) of the MMMs was measured using differential scanning calorimetry (Perkin Elmer, DSC Pyris-1). The membrane sample was cut into small pieces, weighed and placed into a pre-weighed aluminium crucible. The membrane sample was then heated at temperature ranges of 30–350°C at a heating rate of 10°C min^{-1} in the first cycle to remove the thermal history. The sample was then cooled from 350 to 30°C at a cooling rate of 10°C min^{-1}. The same procedure was repeated in the next heating cycle. T_g of the sample was determined as the midpoint temperature of the transition region in the second heating cycle.

Field emission scanning electron microscopic (FESEM) study was made using VPFESEM, model Zeiss Supra55VP. The membrane samples, without coating by silicon rubber, were fractured in liquid nitrogen with the intention of achieving a clean break. The samples were then mounted on a stainless steel stand with carbon tape and coated with 15nm of gold using a sputter coater.

3.0 RESULTS AND DISCUSSION

3.1 Characterization of MMMs using Thermal Gravimetric Analysis

Figure 1 shows the thermogravimetric (TG) curves comparing all types of membranes including neat PSF membrane, PSF/MMT MMM and PSF/O.MMT MMM; while Figure 2(a) and (b) demonstrate the derivative thermogravimetric (DTG) curves for PSF/MMT MMM and PSF/O.MMT MMM, respectively. Thermal stability is an important factor that influenced the structure and morphology of membranes [10]. Therefore, TGA was performed to analyze and compare the thermal stability of the neat PSF membrane and MMMs. The DTG curves show the peak where degradation of the samples occur.

The decomposition temperature of the neat PSF membrane is observed at 541°C. For PSF/MMT MMM, the decomposition was observed at 551°C for PSF/1wt% MMT MMM, 556°C for PSF/3wt% MMT MMM and 554°C for PSF/5wt% MMT MMM. The onset decomposition temperature of the neat PSF membrane was found to be 520±2°C, while PSF/MMT MMMs was at approximately 530±2°C. On the other hand, for PSF/O.MMT MMM, the decomposition temperature corresponded to two peaks: 410°C and 551°C for PSF/1wt% O.MMT, 398°C and 547.5°C for PSF/3wt% O.MMT and 395°C and 558°C for PSF/5wt% O.MMT. Similarly, two onset temperature was found for each curve to be at approximately 360±5°C and 500±5°C. Compared to the neat PSF membrane, all the MMMs exhibited higher decomposition temperature, with PST/5wt% O.MMT MMM showing the highest decomposition temperature (558°C). The two types of MMMs exhibited approximately the same thermal profile.

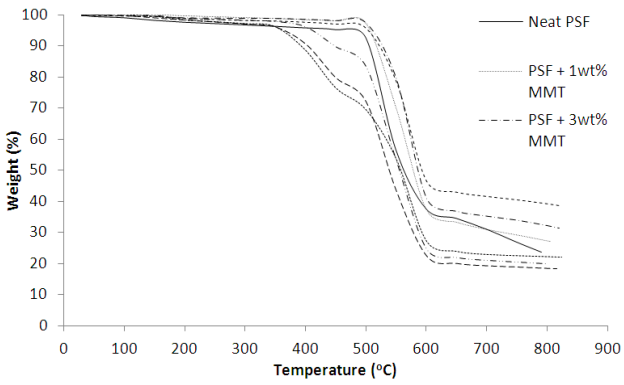

Figure 1 TG curves of the neat PSF membrane, PSF/MMT MMM and PSF/O.MMT MMM

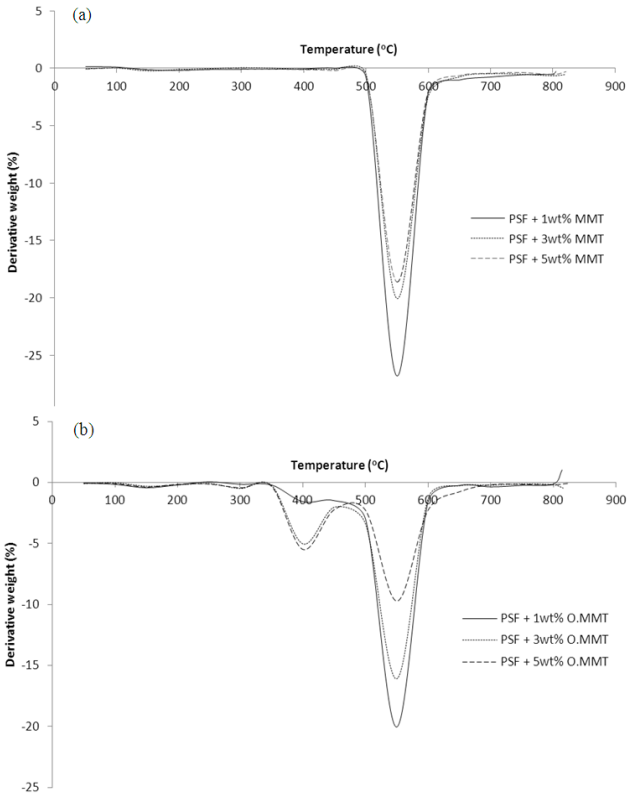

Figure 2 DTG curves of (a) PSF/MMT MMM and (b) PSF/O.MMT MMM

The improvement of the decomposition temperature for all MMMs resulted from the resistance provided by clay's layered morphology which retarded the diffusion of oxygen into the polymer matrix [11]. As the clay loading increases, more heat is absorbed during heating of the MMMs, thus delayed the decomposition. As a result, the decomposition temperature was raised for all MMMs [12]. This behavior is similar with the results reported by Bikiaris where the author suggested that enhanced thermal stability is closely related to the interactions between the clay particles and the polymer matrices [13]. The filler structure acts as mass transport barrier that hinders volatization of decomposed gaseous products via degradation. It has also been found that homogenous dispersion of nanoparticles contribute towards thermal enhancement. In this regard, the particles act as thermal insulation layers with large surface area to protect the polymer chains from decomposition.

Reduction in decomposition temperature of PSF/MMT MMM of 3wt% clay to 5wt% is believed to be due to the formation of agglomerates in the MMM as illustrated by the FESEM images in Figure 3(c) and (d). The inference is in agreement with Bikiaris's study which supported the theory that formation of aggregates may cause thermal stability deterioriation [13].

The two decomposition peaks recorded for PSF/O.MMT is believed to be due to decomposition of the surfactants and the MMT. The first peak depicts the decomposition of the methyl dihydroxyethyl hyrogenated tallow-ammonium surfactant, while the second peak corresponded to the MMT functional group decomposition. Compared with the decomposition temperature of PSF/MMT, the second peak of PSF/O.MMT exhibited approximately the same temperature profile. The inconsistency in the MMM reading is believed to be due to non-homogenous dispersion of clay in the polymer matrix as shown by the FESEM images in Figure 4(e)-(g).

3.2 Characterization of MMMs using Differential Scanning Calorimetry

The glass transition temperature, T_g of the neat PSF membrane, PSF/MMT MMM and PSF/O.MMT MMM is shown in Table 1.

Table 1 Glass transition temperature for the fabricated membranes

Membranes	T_g (°C)
Neat PSF	183.74 ± 0.1
PSF/1wt% MMT	201.62 ± 0.1
PSF/3wt% MMT	207.61 ± 0.1
PSF/5wt% MMT	210.10 ± 0.1
PSF/1wt% O.MMT	217.10 ± 0.1
PSF/3wt% O.MMT	226.08 ± 0.1
PSF/5wt% O.MMT	230.07 ± 0.1

The T_g of all the MMMs is higher than that of the neat PSF membrane. It was found that the introduction of 1wt% MMT into PSF serves to substantially increase the T_g by 9.73%. At 3wt% and 5wt% MMT loading, an even higher T_g over that of PSF is evident. Similar trend was observed for O.MMT loading. This can be explained in terms of exfoliated dispersion of MMT in the polymer matrix [14]. Addition of stiff clay platelets acts as reinforcement to polymer chains at a molecular level; consequently obstructs the localized motions of polymer chains. This resulted in an increase in T_g, signifying that the MMT caused the structure of the membrane to become more crystalline and less amorphous.

3.3 Morphology of Mixed Matrix Membranes

Study on the morphology of the membrane is important to predict the overall membrane performance. Figure 3 shows the FESEM images for the cross section of neat PSF membrane, PSF/ MMT MMMs and PSF/O.MMT MMMs at different clay loading; Figure 4 shows the micrographs of the skin surface. The measured thickness of the membrane is between 60 to 80μm. The thickness and structure of the MMM is closely related to the polymer concentration and viscosity of the casting dope as well as the evaporation rate during casting [15-17].

Thin and porous asymmetric membranes were successfully formed through dry-wet phase inversion technique. The dry phase inversion formed the dense skin layer while wet phase inversion formed the membrane substructure [17]. This structure greatly enhances the productivity of the membrane, in which thin dense skin layer act as selective layer and porous layer act as a support to the skin [18].

Hence, homogenous dispersion of MMT in the selective layer is important since it contributes towards the characteristics of the selective layer. Figure 4 shows the dispersion of the aluminosilicate material nano-clay filler at the skin surface of the MMMs. Fine and homogenous distribution of clay was observed for PSF/MMT MMM as shown in Figure 4(b)-(d). The even distribution of clay is aided by the small nano-sized particle and the sonication process. Study by Aaroon and colleagues concluded that smaller particles such as sub-micron and nano-sized particles will fit in the skin layer better than larger particles [16]. In addition, nano-sized nonporous fillers such as MMT will provide higher polymer-particle interfacial area and improved interface contact. On the other hand, it was found that the organomodified nanoclay dispersed non-homogeneously for PSF/O.MMT MMM as depicted in Figure

4(e)-(g). Figure 4(e) showed initial signs of clay agglomeration. These small agglomerates were found to be distributed unevenly over the entire sample. As O.MMT loading increased, the average size of agglomerates increased as can be seen in Figure 4(f) and (g). Moreover, there appears to be pinholes present on the top surface of the membranes. Formation of air bubbles was observed during the preparation of casting dope which increased with clay loading. Although the dope was degassed, nanoscale air bubbles might be trapped at molecular level.

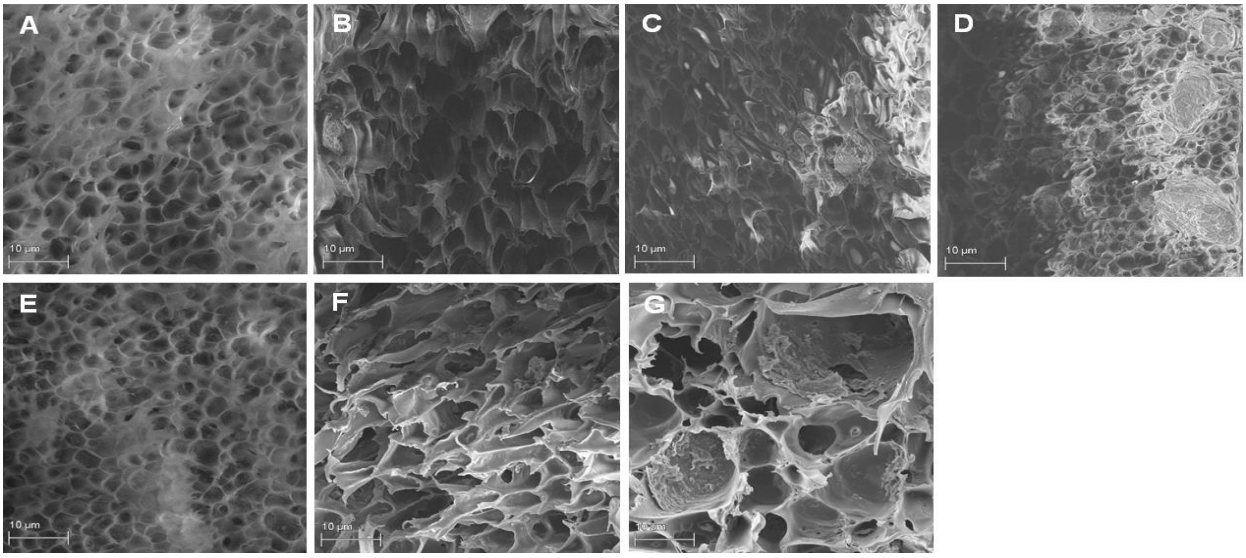

Figure 3 FESEM micrographs for cross sectional view of membranes: (a) neat PSF (b) PSF/1wt% MMT (c) PSF/3wt% MMT (d) PSF/5wt% MMT (e) PSF/1wt% O.MMT (f) PSF/3wt% O.MMT (g) PSF/5wt% O.MMT

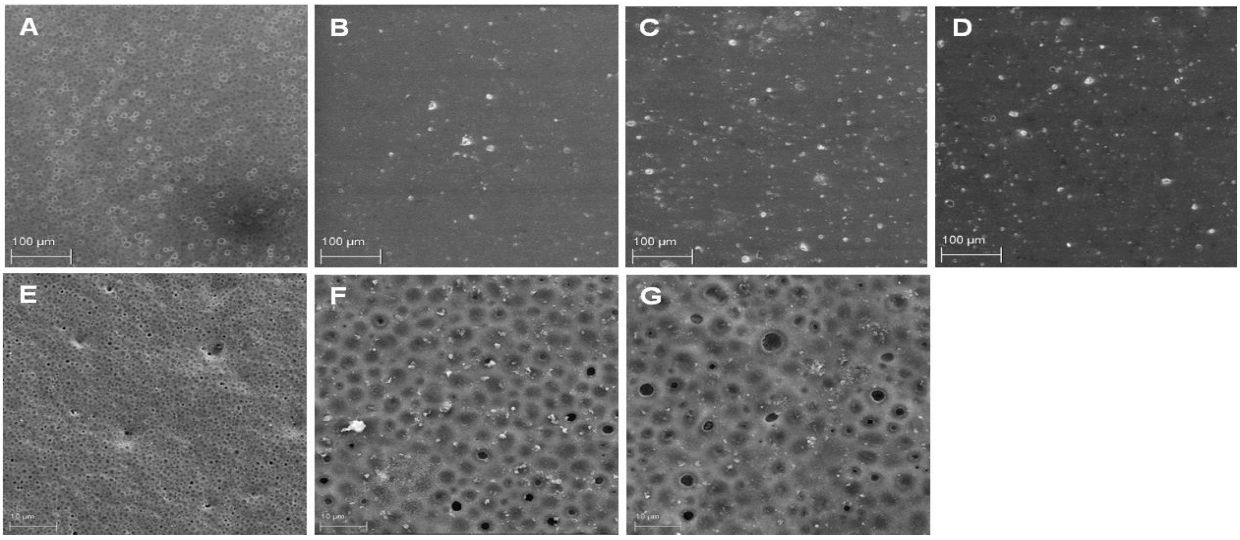

Figure 4 FESEM micrographs for surface view of membranes: (a) neat PSF (b) PSF/1wt% MMT (c) PSF/ PSF/3wt% MMT (d) PSF/5wt% MMT (e) PSF/1wt% O.MMT (f) PSF/3wt% O.MMT (g) PSF/5wt% O.MMT

Figure 3(b) illustrates the morphology of PSF/MMT MMM with 1wt% clay loading. Due to low clay concentration, detecting the MMT particles at the FESEM cross sectional view was a challenge. Interface voids were identified surrounding the clay particles. Weak organic-inorganic interaction caused the voids to form in the polymer-filler interface [19]. Besides, the nucleation of the non-solvent/ polymer around the filler during phase separation process might also contribute to the defects [18].

From Figure 3(c) and (d), particles agglomeration can be observed. As the clay content in the MMM increased, the particle cluster became more significant and bigger agglomerates were formed. Many literatures reported that bigger aggregates caused poor adhesion, consequently larger voids were formed [12, 18, 20-22]. Interestingly, the FESEM result contradicted with the previous studies. MMM with 3wt% and 5wt% of clay content shows better adhesion between PSF and MMT, forming smaller void.

PSF/MMT MMM with 5% mass fraction are believed to have formed rigidified polymer layer around the nanoparticles. The polymer-clay adhesion was good but reduction in free volume is believed to occur around the MMT. Moore and Koros

[23] described interface voids and matrix rigidification as interface defects which resulted from the stresses due to reduction in free volume during solvent evaporation. Voids or 'sieve-in-a-cage' will result in high permeability since gas molecules can pass through the nano-gap between polymer and clay, subsequently reduces selectivity; while rigidified polymer layer will result in higher selectivity, but low permeability.[6] The latter phenomenon is more favourable unless the rigidified polymer permeability is so low that it significantly affects the membrane performance [18].

Figure 3(e)-(g) illustrate the cross sectional FESEM images of PSF/O.MMT. Large pores were observed from the images with higher O.MMT loading as there were less interaction between the polymer matrix and the nanoclay. No significant adhesion between polymer and clay was observed. At higher clay loading, particles agglomeration was found together with large voids between the nanoclay surface and the membrane. The dispersion of the clay was random, forming aggregates at the top, bottom or in the middle layer of the membranes.

■4.0 CONCLUSION

Three types of membranes were fabricated using dry-wet phase inversion method: PSF membrane, PSF/MMT MMM and PSF/O.MMT MMM. The casting dope was prepared at fixed polymer-solvent ratio, while the MMT loading was varied to be 1wt%, 3wt% and 5wt%, respectively. TGA and DSC studies were performed to analyze the effect of nanoclay fillers to the thermal profile of the membranes. The TGA results showed enhancement of thermal stability of MMMs compared to the neat PSF membrane. The study also proved that the thermal stability is influenced by the morphology of the MMM. FESEM was performed to analyze the morphology of all the membrane samples. Thin asymmetric membrane with dense skin layer and porous sub-structure was observed. In order to prove the inference made from the morphology of the MMMs, gas permeation test can be conducted. Based on the reported results, PSF/MMT MMM is expected to have better selectivity and permeability compared to the neat polymer membrane; while PSF/O.MMT will offer good permeability with reduced selectivity. It can be concluded that PSF is not compatible with surface modified MMT with 25-30% of methyl dihydroxyethyl hyrogenated tallow-ammonium.

Acknowledgement

This work was supported by Universiti Teknologi PETRONAS (UTP) under STIRF Grant No. 27/2012 for 2012-2013.

References

[1] Baker, R. W. 2009. Membrane Gas Separation Application. *Membrane Operations: Innovative Separations and Transformations*. 167–194.
[2] Murphy, T. M.; Offord, G. T.; Paul, D. R. 2009. Fundamentals of Membrane Gas Separation. *Membrane Operations: Innovative Separations and Transformations*. 63–82.
[3] Scholes, C. A.; Kentish, S. E.; Stevens, G. W. 2008. Carbon Dioxide Separation through Polymeric Membrane Systems for Flue Gas Applications. *Recent Patents on Chemical Engineering*. 1: 52–66.
[4] Susanto, H.; Unbricht, M. 2009. Polymeric Membranes for Molecular Separation. *Membrane Operations: Innovative Separations and Transformations*. 19–43.
[5] Robeson, L. M. 1991. Correlation of Separation Factor Versus Permeability for Polymeric Membranes. *Journal of Membrane Science*. 62: 165–185.
[6] Cong, H.; Radosz, M.; Towler, B. F.; Shen, Y. 2007. Polymer-Inorganic Nanocomposite Membranes for Gas Separation. *Separation and Purification Technology*. 55: 281–291.
[7] Zimmerman, C. M. 1997. Tailoring Mixed Matrix Composite Membranes for Gas Separation. *Journal of Membrane Science*. 137: 145–154.
[8] Ma, Y.; Shi, F.; Zhao, W.; Wu, M.; Zhang, J.; Ma, J. 2012. Preparation and Characterization of PSF/Clay Montmorillonite Nanocomposite Membranes with LiCl as a Pore Forming Additive. *Desalination*. 39–47.
[9] Sorrentino, A.; Gorrasi, G.; Tortora, M.; Vittoria, V. **2006**. Barrier Properties of Polymer/Clay Nanocomposite *Polymer Nanocomposites*. 273–296.
[10] Leszczynska, A.; Njuguna, J.; Pielichowski, K.; Banerjee, J. 2007. Polymer/ montmorillonite Nanocomposite with Improved Thermal Properties Part I: Factors Influencing Thermal Stability and Mechaninsms of Thermal Stabillity Improvement. *Thermochimica Acta*. 75–96.
[11] Sur, G.; Sun, H.; Lyu, S.; Mark, J. 2001. Synthesis, Structure, Mechanical Properrties, and Thermal Stability of some Polysulfone/ Organoclay Nanocomposites. *Polymer Nanocomposites*. 9783–9789.
[12] Liang, C. Y.; Uchytil, P.; Chkovych, R. P.; Lai, Y. C.; Friess, K.; Sipek, M.; Reddy, M. M.; Suen, S. Y. 2012. A comparison on Gas Separation between PES(polyethersulfone)/MMT (Na-montmorillonite) and PES/TiO2 mixed matrix membranes. *Separation and Purification Technology*. 57–63.
[13] Bikiaris. 2011. Can Nanoparticles Really Enhance Thermal Stability of Polymers? Part II: An Overview on Thermal Decomposition of Polycondensation Polymers. *Thermochimica Acta*. 25–45.
[14] Ranade, A. 2001. Polyamide-imide and Montmorillonite Nanocomposites. University of North Texas.
[15] Barth, C., Goncalves, M., Pires, A., Roeder, J., Wolf, B. 2000. Asymmetric Polysulfone and Polyethersulfone Membrane: Effects of Thermodynamic Conditions during Formation on their Performance. *Journal of Membrane Science*. 287–299.
[16] Aroon, M., Ismail, A., Matsuura, T., Montazer-Rahmati, M. 2010. Morphology and Permeation Properties of Polysulfone Membranes for Gas Separation: Effects of Non-solvent Additives and Co-solvent. *Separation and Purification Technology*. 194–202.
[17] Ismail, A.; Lai, P. 2003. Effects of Phase Inversion Rehological Factors on Formation of Defect-free and Ultraskinned Asymmetric Polysulfone for Gas Separation. *Separation and Purification Technology*. 127–143.
[18] Liu, C., Kulprathipanja, S., Hillock, A. M., Husain, S., Koros, W. J. 2008. Recent Progress in Mixed-Matrix Membranes. *Advanced Membranes Technology and Applications*. 789–819.
[19] Aroon, M., Ismail, A., Montazer-Rahmati, M. 2010. Performances Studies of Mixed Matrix Membranes for Gas Separation: A Review. *Separation and Purification Technology*. 229–242.
[20] Wahab, M., Ismail, A., Shilton, S. 2012. Studies on Gas Permeation Performance of Asymmetric Polysulfone Hollow Fiber Mixed Matrix Membranes using Nanosized Fumed Silica as Fillers. *Separation and Purification Technology*. 41–48.
[21] Anh, J., Chung, W. J., Pinnau, I., Guiver, M. D. 2008. Polysulfone/Silica Nanoparticle Mixed-matrix Membranes for Gas Separation. *Journal of Membrane Science*. 123–133.
[22] Bastani, D.; Esmaeili, N.; Asadollahi, M. 2013. Polymeric Mixed Matrix Membranes Containing Zeolites as a Filler for Gas Applications: A Review. *Journal of Industrial and Engineering Chemistry*. 375–393.
[23] Moore, T. T.; Koros, W. J. 2005. Non-ideal Effects in Organic-Inorganic Materials for Gas Separation Membranes. *Journal of Molecular Structure*. 87–98.